environmental microbiology

Environmental Microbiology (2019) **21**(7), 2559–2575 doi:10.1111/1462-2920.14649

SAR11 bacteria have a high affinity and multifunctional glycine betaine transporter

Stephen E. Noell and Stephen J. Giovannoni*
Department of Microbiology, Oregon State University, Corvallis, OR, USA.

Summary

Marine bacterioplankton face stiff competition for limited nutrient resources. SAR11, a ubiquitous clade of very small and highly abundant *Alphaproteobacteria*, are known to devote much of their energy to synthesizing ATP-binding cassette periplasmic proteins that bind substrates. We hypothesized that their small size and relatively large periplasmic space might enable them to outcompete other bacterioplankton for nutrients. Using uptake experiments with ^{14}C-glycine betaine, we discovered that two strains of SAR11, *Candidatus* Pelagibacter sp. HTCC7211 and *Cand.* P. ubique HTCC1062, have extraordinarily high affinity for glycine betaine (GBT), with half-saturation (K_s) values around 1 nM and specific affinity values between 8 and 14 L mg cell^{-1} h^{-1}. Competitive inhibition studies indicated that the GBT transporters in these strains are multifunctional, transporting multiple substrates in addition to GBT. Both strains could use most of the transported compounds for metabolism and ATP production. Our findings indicate that *Pelagibacter* cells are primarily responsible for the high affinity and multifunctional GBT uptake systems observed in seawater. Maximization of whole-cell affinities may enable these organisms to compete effectively for nutrients during periods when the gross transport capacity of the heterotrophic plankton community exceeds the supply, depressing ambient concentrations.

Introduction

Competition is extreme among osmotrophic bacterioplankton occupying the oligotrophic open ocean. Osmotrophic bacterioplankton live freely suspended in the water column and have access only to the nutrients that diffuse to them, making them reliant on their ability to sequester molecules from the environment at the nutrient concentrations that surround them. In this situation, there are several possible scenarios by which cells can compete. For example, cells may evolve to rapidly transport dissolved compounds during short intervals of peak resource availability, or may use surface enzymes to degrade macromolecules into monomeric compounds that can be transported. However, the simplest strategy a cell can use to compete for nutrients is by transporting them efficiently at ambient concentrations. As an illustration of the ambient oligotrophic conditions facing bacterioplankton in the open ocean, average concentrations of dissolved free amino acids, an important component of dissolved organic matter (DOM), are usually in the low nanomolar range, about 10 times lower than near coasts (Lee and Bada, 1977; Thurman, 1985). Microbes that can more rapidly bind and transport substrates from the environment at these prevailing conditions will, in principle, out-compete other microbes for the nutrients needed for growth.

The SAR11 clade of *Alphaproteobacteria* are among the most successful groups of bacterioplankton in the ocean, making up about a third of all bacterioplankton in surface waters (Morris *et al*., 2002). The success of SAR11 cells has been attributed to their cell-surface properties that enable predator evasion (Dadon-Pilosof *et al*., 2017), specialization in the metabolism of low-molecular-weight compounds, including volatile compounds (Halsey *et al*., 2017) and minimization of cell architecture, which reduces the amount of resources required for replication (Giovannoni, 2005). It has been observed that SAR11 cells devote a large proportion of their energy to producing substrate-binding proteins (SBPs) for ATP-binding cassette (ABC) transporters (Sowell *et al*., 2009). Unlike TonB transporters, which are more common in *Gammaproteobacteria* (Tang *et al*., 2012), ABC transporters utilize periplasmic SBPs, which first bind the substrate before interacting with the transmembrane transporter protein (Bosdriesz *et al*., 2015). SAR11 cells have large periplasmic spaces, making up 25%–35% of cell volume (Nicastro *et al*., 2006). According to theory developed by Bosdriesz *et al*. (2015), the production of large numbers of SBPs by SAR11 cells

Received 30 January, 2019; accepted 6 May, 2019. *For correspondence. E-mail steve.giovannoni@oregonstate.edu; Tel. (541) 737-1835; Fax (541) 737-0498. [Correction added on 28 June 2019, after first online publication: The chemical compound 'alanine betaine' has been corrected to 'trimethylalanine' throughout this version.]

should increase the probabilities that diffusing substrates will be bound, thus increasing transport rates and affinities.

The Michaelis–Menten kinetic parameter K_s is sometimes used to compare whole-cell affinities of bacteria for their substrates. K_s is the half-saturation constant, defined as the concentration of substrate (S) where the uptake rate of S is half of the maximum uptake rate (V_{max}). K_s is a measure of the concentration of S that is saturating for the transporter and so measures the concentrations at which a transporter functions efficiently (Button, 1998). Most reported values of K_s for bacterial transport of specific organic substrates by individual species are in the micromolar range (Schut *et al*., 1995; Lendenmann *et al*., 1996; Button *et al*., 1998; Choquet *et al*., 2005). However, the reported K_s values for bulk marine microbial communities for organic substrates are in the picomolar to nanomolar range (Kiene and Williams, 1998). The cells responsible for these low K_s transport functions in the ocean have yet to be identified.

Specific affinity (a^o_S) is a more wholistic measure of affinity than K_s. The whole-cell uptake kinetics of microbial cells have been found to deviate from traditional Michaelis–Menten kinetics, due to the presence of cellular components that can affect kinetics (e.g., porin size and number, SBP number, cell surface area, etc.) (Koch and Wang, 1982; Button *et al*., 2004; Flynn *et al*., 2018). Button developed the concept of a^o_s to describe the ability of whole cells to sequester substrates, with more efficient oligotrophs having higher a^o_s values (Button, 1998). a^o_s is calculated from V_{max}/K_s (Button, 1998). V_{max} and K_s are determined experimentally by measuring uptake rates (V) at a range of concentrations and using nonlinear modelling to fit the Michaelis–Menten equation to a plot of V versus S (Greco and Hakala, 1979). As V_{max} measurements require accurate biomass measurements, which can be difficult and time-consuming (Cermak *et al*., 2017), K_s is often used instead of a^o_s to compare the affinities of different species (Flynn *et al*., 2018).

In this paper, we set out to determine how the most abundant lineage of SAR11 cells, *Pelagibacter*, compare with other bacteria in their ability to sequester nutrients from the environment. We hypothesized that *Pelagibacter* cells would have high a^o_s values and low K_s values for organic substrates compared with other bacteria, given the large percentage of their proteome devoted to transporters and their success in oligotrophic surface waters around the world (Morris *et al*., 2002; Sowell *et al*., 2009). We also hypothesized that SAR11 transporters are multifunctional, capable of transporting numerous structurally similar compounds and metabolizing them. We based this hypothesis on the observation that SAR11 cells have highly streamlined genomes, among the smallest for a free-living organism (1.3 Mbp), yet are highly successful in oligotrophic ecosystems (Giovannoni, 2005). *Pelagibacter* cells have been shown to have multifunctional enzymes before (Green *et al*., 2011; Ferla *et al*., 2017). In obligate pathogenic and endosymbiotic bacteria, a reduction in genome size has been found to be associated with an increased functional complexity in enzymes (Kelkar and Ochman, 2013). It is possible that a similar evolution towards increased multifunctionality has enabled bacteria with streamlined genomes, such as SAR11, to thrive in the open ocean. *Pelagibacter* cells have unique growth requirements, specifically glycine, pyruvate, a reduced sulfur source and vitamins (Carini *et al*., 2013). As these compounds are found in low concentrations in the ocean and have high turnover rates (Obernosterer *et al*., 1999; Kiene and Linn, 2000; Carini *et al*., 2014; Lu *et al*., 2014), it has been suggested that *Pelagibacter* cells are able to substitute a variety of compounds to meet their unique requirements, but the full range of substitutable compounds has not been determined (Giovannoni, 2017).

For this work, we used glycine betaine (GBT) as the organic substrate. GBT is used by cells either for osmotic regulation (Rudulier and Bouillard, 1983) or as a glycine source (King, 1984; Diaz *et al*., 1992). GBT is known to be produced by marine phytoplankton (Kiene *et al*., 1998; Keller *et al*., 1999), can substitute for glycine in *Pelagibacter* growth (Carini *et al*., 2013) and is transported and metabolized by marine bacterioplankton in general (Kiene *et al*., 1998). The GBT ABC transporter is one of the top 25 most abundant transport proteins expressed by SAR11 cells (Sowell *et al*., 2009). Marine bacterioplankton have been observed to have promiscuous GBT transporters, with osmolytes similar in structure to GBT, such as dimethylsulfoniopropionate (DMSP), choline, and proline betaine, showing moderate to strong competition for the GBT transporter (Kiene *et al*., 1998). *Pelagibacter* cells are known to oxidize several common osmolytes, including DMSP, an osmolyte known to be produced by phytoplankton and bacteria (Sun *et al*., 2016; Curson *et al*., 2017), and taurine, an osmolyte known to be secreted by zooplankton (Carini *et al*., 2013; Clifford *et al*., 2017).

Our research strategy is to explore ecologically relevant metabolic processes with genomes, cell cultures and field experiments (Sun *et al*., 2011; Halsey *et al*., 2017; Giovannoni *et al*., 2019). This approach addresses properties of cells that are not predictable from omics data but contribute to activities observed at the ecosystem level. We studied two *Pelagibacter* strains, HTCC1062 and HTCC7211, which represent the 1a.1 and 1a.3 ecotypes of *Pelagibacter* respectively. Their biogeographical distributions vary with latitude: the 1a.1 ecotype is found in cool temperate and polar waters, whereas the 1a.3 ecotype is abundant in warm equatorial and sub-tropical waters (Brown *et al*., 2012). In some temperate regions, these two ecotypes oscillate seasonally (Eren *et al*., 2013). We measured whole-cell transport kinetics for GBT and congeneric

compounds, demonstrating superior transport kinetics and multifunctionality in this transport system. We then showed that the cells were able to use many of the transported organic substrates as substitutes for growth requirements.

Results

Kinetics experiments. The best-fit Michaelis–Menten non-linear regression model for uptake of GBT had a correlation value of 0.86 for HTCC1062 and 0.95 for HTCC7211 (Fig. 1). V_{max} was calculated to be 12.60 nmoles mg cells^{-1} h^{-1} (1.48 μg S mg cells^{-1} h^{-1}) for HTCC1062 and 14.92 nmoles mg cells^{-1} h^{-1} (1.75 μg S mg cells^{-1} h^{-1}) for HTCC7211. K_s was calculated to be 0.89 nM (0.104 μg S L^{-1}) for HTCC1062 and 1.85 nM (0.217 μg S L^{-1}) for HTCC7211. The calculated a°_s from these values, using V_{max}/K_s, is 14.2 L mg cells^{-1} h^{-1} for HTCC1062 and 8.06 L mg cells^{-1} h^{-1}for HTCC7211. These values are higher than most reported specific affinity values for bacterial species and a single organic substrate (Table 1), but are lower than the highest ever-reported value, which is 20 L mg cells^{-1} h^{-1} for the marine bacterium *Cycloclasticus oligotrophus*, substrate toluene (Button *et al*., 1998).

The measured K_s values for HTCC1062 and HTCC7211 with GBT are extraordinarily low, indicating that substrate saturation occurs at very low concentrations. The measured K_s values are the lowest that we could find for a pure cultured microbe and its organic substrate (Table 1). On the other hand, the V_{max} values of both SAR11 strains are lower than other reported values for V_{max} and are far below the highest reported values for V_{max} in Table 1. V_{max} values are difficult to measure for environmental samples, as the biomass of the microbial community and background concentrations of the substrate are generally unknown, making it difficult to compare the measured V_{max} values from this study to environmental values. One of the few V_{max} values reported for seawater (with leucine as the substrate) was calculated to be 45.74 nmoles mg cells^{-1} h^{-1}, which is closer to the values measured for *Pelagibacter* cells (13–15 nmoles mg cells^{-1} h^{-1}) than values measured for other axenic cultures of bacteria from Table 1, all except two of which are above 500 nmoles mg cells^{-1} h^{-1} (Button, 1998).

Competition assay. To determine the compounds that could compete for uptake via the GBT transporter in *Pelagibacter* cells, a competition assay was used, where unlabelled competitor compounds were added to *Pelagibacter* cells in addition to ^{14}C-GBT (Fig. 2). A list of competitor compounds used, along with their chemical characteristics, is given in Table 2. The ^{14}C-GBT uptake in the competitor treatments was calculated as a percentage of ^{14}C-GBT uptake in the 'None' control that had no competitor compounds added. In both strains of *Pelagibacter*, the positive control with unlabeled GBT as the competitor showed a significant decrease ($P < 0.05$, one-sided Dunnett's test) in ^{14}C-GBT uptake, with only 14% or 25% (HTCC1062 or HTCC7211 respectively) of the uptake observed in the 'None' control (Fig. 2). In both strains, the negative control with glucose as competitor showed about 85% of the uptake in the 'None' control.

In HTCC1062, addition of nine compounds (not including the positive control) was found to result in a significant decrease ($P < 0.05$, one-sided Dunnett's test) in uptake compared with the negative control, indicating competition for the same transporter as the ^{14}C-GBT (Fig. 2). In HTCC7211, only six competitors were significant competitors ($P < 0.05$, one-sided Dunnett's test). Out of those six, five were also significant competitors for ^{14}C-GBT in HTCC1062. The sixth significant competitor in HTCC7211, butyrobetaine, was not a significant competitor in

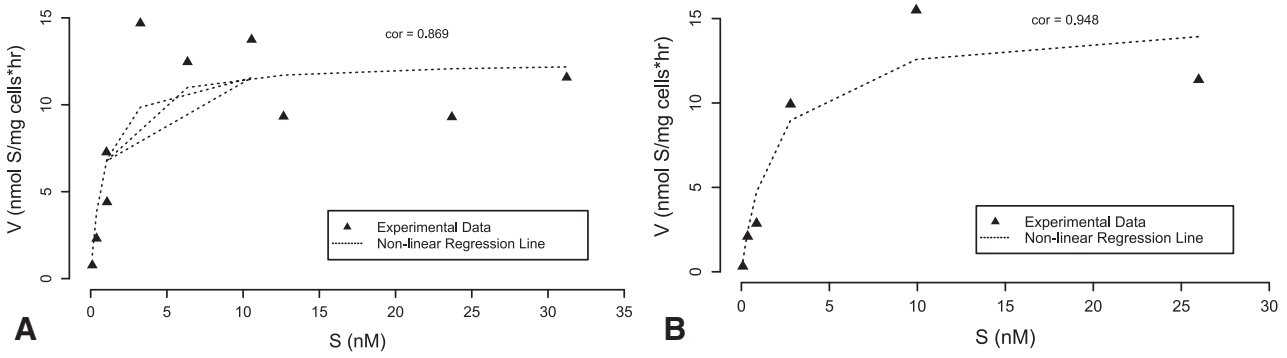

Fig. 1. Uptake rate versus substrate concentration for ^{14}C-glycine betaine (^{14}C-GBT) uptake by (A) HTCC1062 and (B) HTCC7211 cells. Cells were grown to mid-exponential phase, harvested and washed via centrifugation, starved for 2 h and incubated with varying concentrations of ^{14}C-GBT. Uptake was measured at 0, 5 and 10 min using azide and ice to stop uptake, filtration to capture cells, and liquid scintillation to count ^{14}C levels in the cells. Linear regression was used to calculate the uptake rate (V) at each concentration, normalized by biomass (see Methods for conversion factors used). Results from separate experiments are shown in the same plot. Non-linear regression was used to fit a Michaelis–Menten equation to the data. From this regression, for HTCC1062, the maximum uptake rate (V_{max}) was calculated to be 12.60 nmoles mg cells^{-1} h^{-1} (1.48 μg S mg cells^{-1} h^{-1}) and for HTCC7211, 14.92 nmoles mg cells^{-1} h^{-1} (1.75 μg S mg cells^{-1} h^{-1}); the half-saturation constant (K_s) was calculated to be 0.89 nM (0.104 μg S/L) for HTCC1062 and 1.85 nM (0.217 μg S/L) for HTCC7211; the calculated specific affinity (a°_s) from these values, using V_{max}/K_s, is 14.2 L mg cells^{-1} h^{-1} for HTCC1062 and 8.06 L mg cells^{-1} h^{-1} for HTCC7211.

Table 1. Comparison of kinetic constants for the uptake of organic substrates by microbes, in order of increasing K_s values.

Species	Substrate	K_s (nM)	V_{max} (nmol mg cells^{-1} h^{-1})	Specific affinity (L mg cells^{-1} h^{-1})	Reference
Seawater, bay samples	GBT	0.86	-	-	(Kiene and Williams, 1998)
C. P. ubique HTCC1062	GBT	0.89	12.63	14.2	This study
C. P. ubique HTCC7211	GBT	1.85	14.92	8.06	This study
Seawater samples	Glucose	2.3	-	-	(Azam and Hodson, 1981)
Marinobacter arcticus	Glutamate	10.6	23.1	0.373	(Button *et al*., 2004)
Seawater, Resurrection Bay	Leucine	19.82	45.74	2.31	(Button, 1998)
Seawater, estuary samples	Toluene	20.62	-	-	(Button *et al*., 1998)
Oligotrophic marine bacterium strain LNB-155	Glucose	40	-	-	(Nissen *et al*., 1984)
Soil enrichment culture	Methane	56	-	-	(Dunfield *et al*., 1999)
Rhizobium leguminosarum	L-histidine	78	29.3	0.375	(Hosie *et al*., 2002)
E. coli	Ribose	277.5	2819.6	8.5	(Lendenmann *et al*., 1996)
Pseudomonas sp. strain T2	Toluene	477.5	1519.4	3.2	(Button, 1998)
Cycloclasticus oligotrophus	Toluene	651.2	13023.7	20	(Button, 1998)
Marine ultramicrobacterium strain RB2256	Alanine	1300	1200	0.923	(Schut *et al*., 1995)
Erwinia chrysanthemi	GBT	1600	968.4	0.605	(Choquet *et al*., 2005)
L. monocytogenes	L-carnitine	10 000	505.3	0.051	(Verheul *et al*., 1995)

Substrate concentrations were converted into molarity to permit direct comparisons of K_s and V_{max}. Specific affinity values were calculated using the formula V_{max}/K_s in all cases. Where necessary, cell biomass values were converted into milligrams of wet weight using the conversion factors 3 g wet weight g^{-1} dry weight, 5.7 g wet weight g^{-1} protein and 0.55 g carbon g^{-1} dry weight (Martens-Habbena *et al*., 2009).

HTCC1062, likely due to the loss of one of the replicates during the experiment with HTCC1062.

All compounds that showed significant competition with GBT share structural similarities (Table 1). They are all zwitterions, having a negatively charged carboxylic acid at one end and a positive charge at the other (either N or S). However, they differ in the number of carbons separating the positive and negative ends, the presence of a five- or six-member ring or the addition of various functional groups (alcohol or methyl). They also have a range of pKas (1.8–4.2) and molecular weights (117–160 g mol^{-1}). No connection was observed between chemical properties of the compounds and strength of competition.

ATP assay. Both strains of SAR11 were able to use several of the GBT congeneric compounds as ATP sources (Fig. 3). In HTCC1062, addition of four of the eleven compounds tested (DMSP, ectoine, L-carnitine and propionobetaine) resulted in cellular ATP levels significantly above that of the negative control (no added compound) based on a one-sided Dunnett's test ($P < 0.05$). Addition of four other compounds (betonicine, GBT, proline betaine and trigonelline) resulted in cellular ATP levels that were greater than the negative control, but that difference was not significant ($P = 0.31$, 0.19, 0.14 and 0.12 respectively). In HTCC7211, addition of seven of the eleven test compounds (trimethylalanine, betonicine, ectoine, GBT, L-carnitine, propionobetaine and trigonelline) resulted in cellular ATP levels significantly greater than that of the negative control (one-sided Dunnett's test, $P < 0.05$) (Fig. 3).

The ATP levels observed in this study (5–15 ag ATP/cell) are similar to those observed previously for HTCC1062 (5–20 ag ATP/cell) (Steindler *et al*., 2011), but are about 100× larger than those observed in one study with HTCC1062 (Sun *et al*., 2011) and about 100× smaller than those observed for HTCC2181 (400–800 ag ATP/cell), a member of the OM43 group of coastal bacterioplankton (Halsey *et al*., 2012). The ATP contents per cell were higher for HTCC7211 than HTCC1062, likely reflective of the larger cell size of HTCC7211 (Cermak *et al*., 2017).

Growth experiments. The competitor compounds in HTCC1062 and HTCC7211 were examined for their potential metabolism as glycine or pyruvate sources using growth experiments, where the compounds were substituted for either glycine or pyruvate in ASW media and the resulting growth compared with a negative control with no pyruvate or glycine (Fig. 4). Both maximum cell density and growth rate were measured and reported. Treatments where both the maximum cell density and growth rate were significantly higher than the negative control (one-sided Dunnett's test, $P < 0.05$) are referred to as 'strong' substitutes, while treatments where only one of the two metrics were significantly higher than the negative control are referred to as 'weak' substitutes. Some compounds, when added at higher concentrations, resulted in growth rates below that of the negative control. For those compounds (proline betaine, trigonelline, ectoine, propionobetaine, L-pipecolate and butyrobetaine), the added concentrations were lowered until no inhibition of growth was observed (100 nM final concentration).

In HTCC1062, five compounds were strong pyruvate substitutes, with both the growth rate and maximum cell density being significantly higher than the negative control (one-sided Dunnett's test, $P < 0.05$): trimethylalanine, betonicine, L-carnitine, trigonelline and ectoine (Fig. 4 and Supporting Information Tables S3 and S4). In HTCC7211,

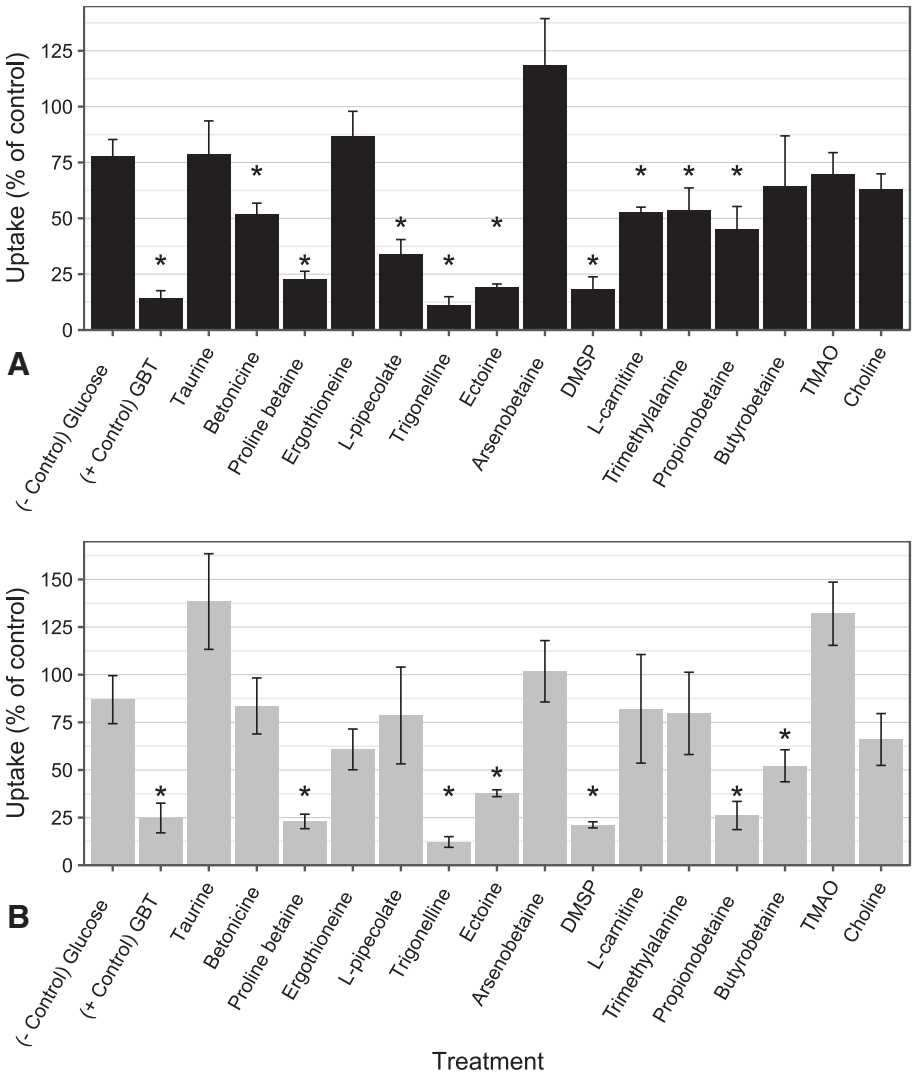

Fig. 2. Competition screening experiment to identify compounds that compete with GBT for uptake in (A) HTCC1062 and (B) HTCC7211. Cells were harvested and washed in mid-exponential phase, and then incubated with ^{14}C-GBT and an unlabelled competitor compound (or no competitor, in the case of the 'None' control) for 10 min. Glucose was used as a negative control and unlabelled GBT as a positive control. Uptake in all treatments was calculated as a percentage of uptake of ^{14}C-GBT in the 'None' control. Treatments are ordered by increasing pKa value for the compound used. Stars indicate significantly lower uptake of ^{14}C-GBT than in the glucose negative control for that species ($P < 0.05$, one-sided Dunnett's test). Error bars represent the standard deviation of triplicate samples.

betonicine was a weak pyruvate substitute, with cultures having a maximum cell density (but not growth rate) significantly greater than the negative control (Fig. 4 and Supporting Information Tables S3 and S4).

As expected, GBT was a strong glycine substitute in both strains (Fig. 4 and Supporting Information Tables S3 and S4). In HTCC1062, propionobetaine was the only other strong glycine substitute. Butyrobetaine and betonicine were both weak glycine substitutes, with growth rates (but not maximum cell densities) that were significantly higher than the negative control. In HTCC7211, L-carnitine and trimethylalanine were both weak glycine substitutes, with cultures having growth rates (but not maximum cell densities) significantly greater than the negative control (0 and -0.02 day^{-1} for L-carnitine and trimethylalanine, respectively, compared with -0.09 day^{-1} for the negative control).

Bioinformatics. The competition assay data indicated differences between the two strains in the GBT SBP-binding specificity, as four of the competitor compounds in HTCC1062 were not significant competitors in HTCC7211 (trimethylalanine, betonicine, L-carnitine and L-pipecolate) (Fig. 2). A phylogenetic tree was constructed for the SBP gene for the GBT ABC transporter in SAR11, *proX*, using sequences from SAR11 subgroup 1a.1 and 1a.3 (Supporting Information Fig. S1). The phylogenetic tree branching order indicated vertical inheritance of *proX*, with clear divergence between the 1a.1 and 1a.3 subgroups. We further investigated *proX* amino acid sequence divergence between the 1a.1 and 1a.3 ecotypes, using a multiple-sequence alignment (MSA), finding conserved amino acid differences between the two subgroups of SAR11 strains (Supporting Information Fig. S2). We used SWISS-MODEL to identify the closest matching protein structure to SAR11 *proX* and aligned the *proX* sequences from HTCC1062 and HTCC7211 to the template. We reasoned that, if the binding specificity of *proX* is different between the 1a.1 and 1a.3 ecotypes,

Table 2. Chemical characteristics of compounds used in competition assay, ordered by increasing pKa value.

Competitor compound	pKa	Molecular weight (g mol^{-1})	Structure
Taurine	0.96	125.15	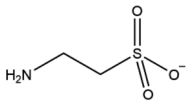
GBT	1.84	117.15	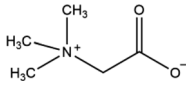
Betonicine	2.06	159.18	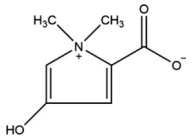
Proline betaine	2.26	143.18	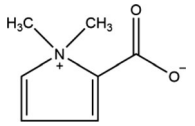
Ergothioneine	2.49	229.3	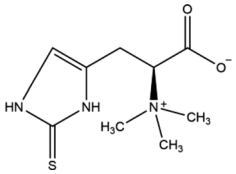
L-pipecolate	2.51	129.16	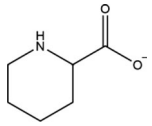
Trigonelline	2.78	137.14	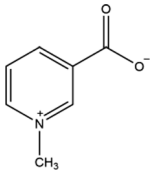
Ectoine	2.87	142.16	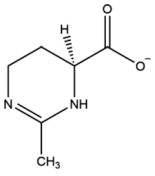
Arsenobetaine	2.90	178.0	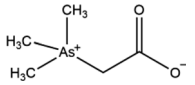
DMSP	3.35	134.20	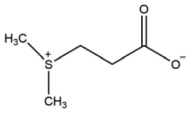

(Continues)

Table 2. Continued

Competitor compound	pKa	Molecular weight (g mol^{-1})	Structure
L-carnitine	4.20	161.19	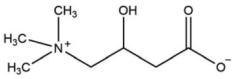
N,N,2-trimethylalanine	2.02	131.17	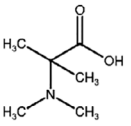
Propionobetaine	4.24	130.2	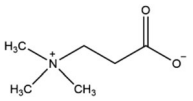
Butyrobetaine	4.46	145.20	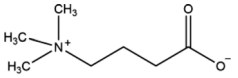
TMAO	4.66	75.1	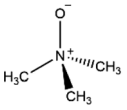
Glucose	11.8	180.16	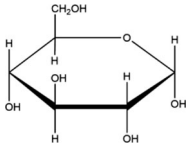
Choline	13.9	104.17	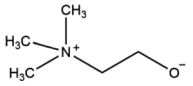

DMSP: dimethylsulfoniopropionate. TMAO: trimethylamine N-oxide

then we would expect to see conserved variation in the ligand-binding pocket in the protein model. The variant amino acid positions were not within 4 Â of the ligand, GBT, and were concentrated in an alpha helix below the binding pocket, indicating these variant residues are likely not involved in ligand binding (Supporting Information Fig. S3).

Discussion

Kinetics experiments. The very low K_s (around 1 nM) and large a^o_s (14.2 L mg cells^{-1} h^{-1} for HTCC1062, 8.06 L mg cells^{-1} h^{-1} for HTCC7211) values for *Pelagibacter* cells indicate that these organisms are adapted to competing for GBT at extremely low nutrient concentrations (Fig. 1). The maximum a^o_s value for *Pelagibacter* cells may be even higher, as experimental procedures have been reported to depress V_{max} values (Robertson and Button, 1979; Flynn, 1998). In addition, the highest reported a^o_s values were

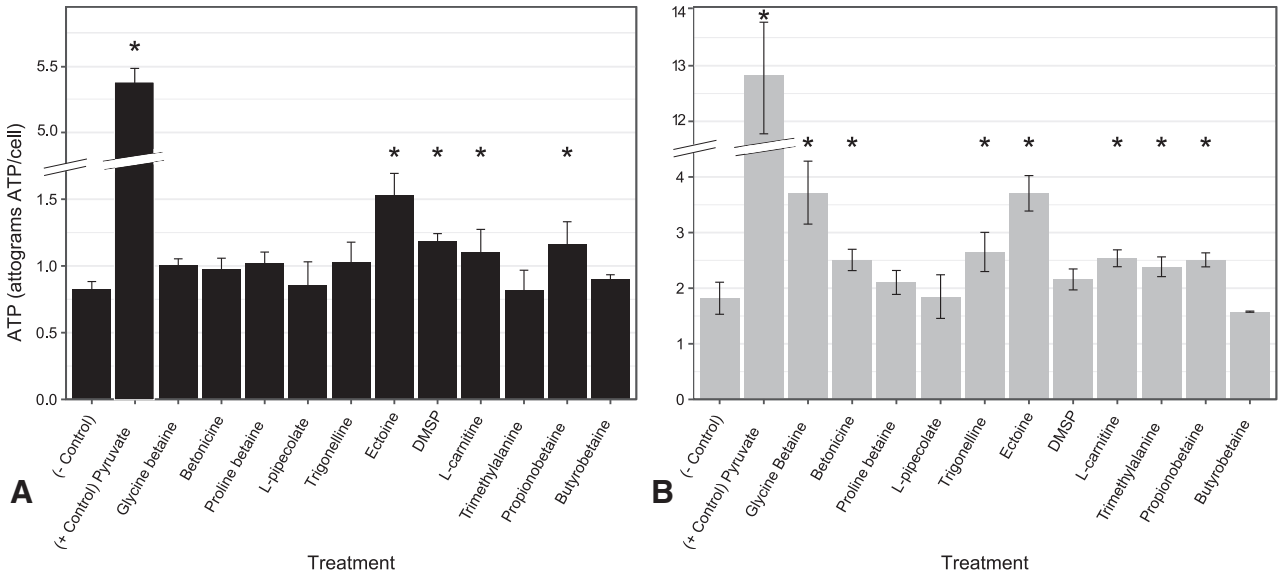

Fig. 3. Intracellular ATP response to organic compound addition, for two SAR11 strains. ATP contents of starved (A) HTCC1062 or (B) HTCC7211 cells were measured via luminescence 5 h after addition of 100 μM pyruvate (positive control to ensure cell activity), no addition (negative control), or one of 11 test compounds. GBT, DMSP, trimethylalanine, L-carnitine, betonicine, trigonelline and ectoine were added at 1 μM final concentration, while propionobetaine, proline betaine, L-pipecolate and butyrobetaine were added at 100 nM, since at higher concentrations, ATP levels decreased below the negative control. Treatments are ordered by increasing pKa value for the compound used. Error bars represent the standard deviation of triplicate cultures. The asterisk indicates that the ATP levels in the treatment were significantly greater than those in the negative control (one-sided Dunnett's test, $P < 0.05$).

measured using very low biomass samples that were sampled from continuous cultures (Button, 1998). *Pelagibacter* cultures in these experiments were not grown with GBT prior to washing, as *Pelagibacter* cells are known to constitutively express most carbon metabolism genes (Sun *et al*., 2011).

The K_s values we report for *Pelagibacter* are the lowest reported for any microbe in pure culture with an organic substrate (excluding micronutrients such as vitamins) (Table 1). *Pelagibacter* K_s values are in the range of reported K_s values from bulk seawater samples with a variety of organic

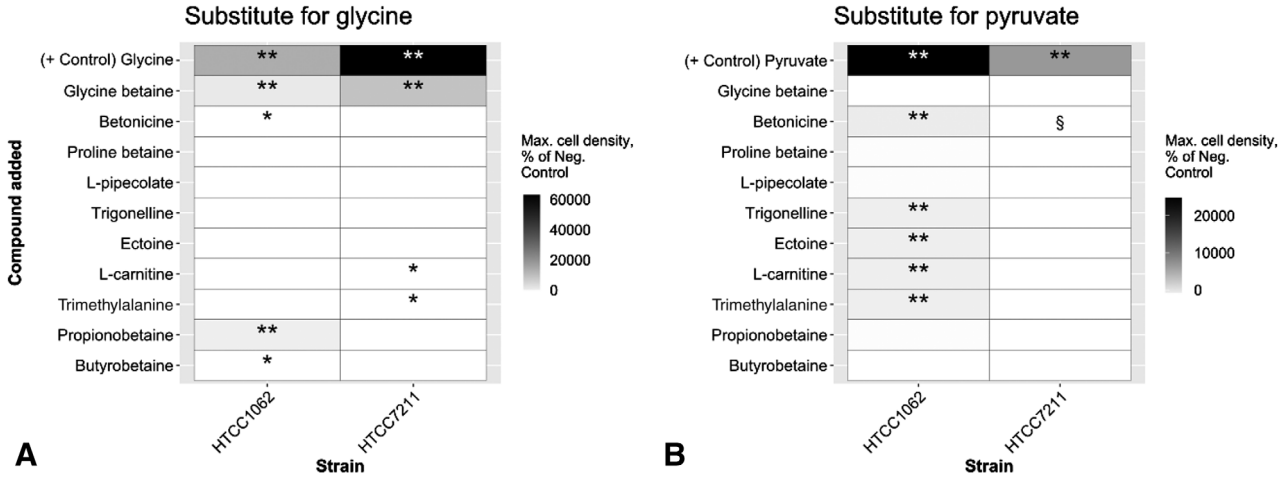

Fig. 4. Growth experiments were used to determine if the competitor compounds substitute for glycine or pyruvate in HTCC1062 and HTCC7211. Either 100 μM pyruvate or 50 μM glycine, 25 μM methionine, and 1× vitamin mix were added to all cultures in addition to either 50 μM (positive control, trimethylalanine, L-carnitine and betonicine), 1 μM (GBT) or 100 nM (proline betaine, trigonelline, ectoine, propionobetaine, L-pipecolate and butyrobetaine) of the test compound. For some compounds, lower concentrations were used if higher concentrations inhibited growth below the negative control. The maximum cell densities shown were calculated as a percentage of the maximum cell densities of negative control cultures with no glycine or no pyruvate added. Treatments are ordered by increasing pKa value for the compound used. A one-sided Dunnett's test was used to determine if the maximum cell density or growth rate in each treatment was higher than the negative control for that experiment ($P < 0.05$). The double asterisk indicates that both the maximum cell density and growth rate for a treatment were significantly higher than in the negative control. The section symbol indicates that only the maximum cell density was significantly greater than the negative control. The asterisk indicates that only the growth rate was significantly higher than the negative control. Raw data for average maximum cell densities and growth rates are given in Supporting Information Tables S1–S4.

substrates (between 1 and 20 nM for GBT, glucose, leucine and toluene), and are almost identical to those observed by Kiene and Williams using bulk seawater samples and GBT as the substrate (Kiene and Williams, 1998). This same study observed that cells in the size range 0.2–1.0 μm, which includes *Pelagibacter* (Giovannoni, 2017), were responsible for a majority (63%) of the observed GBT uptake in seawater samples. Thus, SAR11 cells were likely responsible for the GBT uptake observed in that study.

The very low K_s and high a^o_s values for GBT in *Pelagibacter* cells are likely related to the reliance of these organisms on ABC transporters. ABC transporters are often the prominent transport strategy in Gram-negative cells, allowing them to proliferate SBPs in the periplasm, relative to the number of membrane sites, which are limited by the cell membrane surface area. This alters the probability of binding substrate molecules that enter the periplasm, raising the effective substrate concentration by increasing the number of SBP-substrate complexes (Bosdriesz *et al*., 2015). SAR11 cells have been shown to allocate a large percentage of their proteome to SBPs, in both culture and the environment (Sowell *et al*., 2008, 2009). The high ratio of SBPs to other proteins in SAR11 is related to their small cell volumes, which range from 0.025 to 0.045 μm^3 (Giovannoni, 2017). The high surface-area-to-volume ratio of these cells likely results in a competitive advantage in nutrient acquisition in oligotrophic systems (Nicastro *et al*., 2006; Flynn *et al*., 2018). As much as 35% of *Pelagibacter* cell volume is periplasm in stationary phase (Nicastro *et al*., 2006), compared with 8% to 16% in *Escherichia coli* cells (Graham *et al*., 1991). These features of cytoarchitecture appear to be adaptations that can partly explain the effectiveness of *Pelagibacter* in transporting DOM resources.

It is notable that the V_{max} values for the two SAR11 strains we studied (12.6 and 14.9 nmol mg $cells^{-1}$ h^{-1} for HTCC1062 and 7211 respectively) are the lowest among the values in Table 1. However, they are quite similar to rates of DMSP uptake by HTCC1062 calculated from data reported in Sun *et al*. (2016), which are between 11.5 and 28.2 nmoles DMSP mg $cell^{-1}$ h^{-1}. Those experiments were done under different conditions but are suggestive of similarly low rates of DMSP uptake by HTCC1062. Whole-cell V_{max} values are indicative of the transport capacity of cells for that substrate (Button *et al*., 2004). These findings imply that *Pelagibacter* GBT transporters have a low maximum transport rate, and are possibly related to the low maximal growth rates and minimal regulation of carbon metabolism observed in *Pelagibacter* cells (Sun *et al*., 2011).

The specific affinity values we measured for *Pelagibacter* are relatively close to theoretical maximum values calculated using the method of Koch and Wang (1982), who converted measured affinity values into efficiency of uptake (units of s^{-1}) by multiplying by the density of cells. The maximal efficiency of uptake is calculated assuming a spherical cell, regardless of morphology, using the equation $3D/R^2$, where D is the diffusion coefficient of the substrate and R is the radius of the spherical cell. Taking SAR11 cells to be spherical, the radius is calculated to be 2.06×10^{-5} cm, based on a cell volume of 0.037 um^3 (Zhao *et al*., 2017). The diffusion coefficient for GBT has been measured to be 9.4×10^{-7} cm^2 s^{-1} (Grant and Blackband, 2002). Thus, the theoretical maximal efficiency for *Pelagibacter* cells is 6645 s^{-1}. The measured efficiency of uptake, calculated as above using the specific affinity, was 3932 s^{-1} for HTCC1062 and 2240 s^{-1} for HTCC7211. These measured values are 60% and 34% of the theoretical maximum respectively. These values are closer to the theoretical maximum than other measured uptake efficiencies: 3.83 s^{-1} for a *Pseudomonas* sp. growing on lactate (0.04% of the theoretical maximal value of 9250 s^{-1}) (Koch and Wang, 1982); 54 s^{-1} for *E. coli* with glucose as the substrate (2% of the theoretical maximal value of 2800 s^{-1}) (Koch and Wang, 1982); 5600 s^{-1} for *Cycloclasticus oligotrophus*, the microbe with the highest measured specific affinity, with toluene as the substrate (20% of the theoretical maximal value of 28 700 s^{-1}) (Button *et al*., 1998). These calculations illustrate that *Pelagibacter* cells are operating closer to the maximum theoretical transport efficiency than other microbes.

Specificity of the GBT transporter in SAR11. Enzyme–substrate interaction has long been thought to be specific, as the lock and key analogy of Emil Fischer postulated (Fischer, 1894). This model of enzyme specificity has recently been challenged, with multifunctionality being postulated to be the rule, not the exception, to enzyme functionality (Ferla *et al*., 2017). SBPs in bacterial ABC transporters are usually thought of having high affinity and specificity for their substrates. There are some ABC transporters that have a broader substrate range than average, including some amino acid, maltose and oligopeptide SBPs, and the *opuABC* GBT transporter systems in *Bacillus subtilis* (Schiefner *et al*., 2004; Davidson *et al*., 2008; Hoffmann and Bremer, 2017). The *opuABC* GBT transporter in *B. subtilis* is known to transport 15 separate substrates, including GBT; however, such multifunctionality is unusual for an ABC SBP (Hoffmann and Bremer, 2017).

The GBT transporters in HTCC1062 and HTCC7211 can transport at least 10 and 7 different substrates, respectively, including GBT (Fig. 2). The *proX* SBP in *E. coli*, which the SAR11 GBT transporter is more closely related to (Lidbury *et al*., 2014), is known to bind several substrates with high affinity (K_s = 1.3 μM), including GBT, ectoine and proline betaine (Jebbar *et al*., 1992; Lucht and Bremer, 1994; Schiefner *et al*., 2004). Comparatively, the SAR11 *proX* SBP is much higher affinity and much more multifunctional than its *E. coli* homologue.

The competitive inhibition we observed likely stems from competition for binding to the SBP, as opposed to different SBPs competing for the same permease membrane component. This is evidenced by the presence of only one GBT SBP in the HTCC1062 and HTCC7211 genomes, *proX* (WP_006997122.1 in HTCC1062, WP_008545035.1 in HTCC7211). The other SBP in the HTCC1062 genome annotated as a "glycine/betaine ABC transporter SBP" is *opuAC* (WP_006997986.1), identified by Lidbury *et al*. (2014) as being a homologue to the trimethylamine N-oxide (TMAO) SBP in *Ruegeria pomeroyi.* As TMAO was not one of the compounds that showed competition with GBT for uptake by HTCC1062 or HTCC7211, it seems likely that the *proXYZ* ABC transporter system is solely responsible for the multifunctional transport of GBT in SAR11 cells.

ATP experiments. Having determined that several of the compounds used were competing for uptake, we tested whether *Pelagibacter* cells could use these compounds as energy sources. One of the competitor compounds, DMSP, is already known to be used by HTCC1062 cells as a reduced sulfur source (Sun *et al*., 2016). However, the metabolism of most of the competitor compounds had not been studied in *Pelagibacter. Pelagibacter* cells are unique in that they have requirements for a reduced sulfur source, glycine and pyruvate, and thus cannot be grown on a compound as a sole carbon source (Sun *et al*., 2011). ATP assays were used to determine if starved *Pelagibacter* cells were stimulated to produce ATP by the addition of the significant competitor compounds from Fig. 2.

In HTCC1062, at least four compounds (DMSP, ectoine, L-carnitine and propionobetaine) stimulated ATP levels (Fig. 3). Addition of four other compounds (GBT, proline betaine, betonicine and trigonelline) resulted in ATP levels above the negative control, but that difference was not significant based on Dunnett's test (Fig. 3). As previous studies have found that HTCC1062 cells use GBT for ATP, that result was likely a false-negative. During method development, the trigonelline and betonicine treatments usually had higher ATP levels than the negative control, with a significant difference for trigonelline in several experiments (P = 0.048 and 0.01, one-sided Dunnett's test; data not shown). Proline betaine rarely increased ATP and the increase was never significant (data not shown).

In HTCC7211, seven of the eleven compounds tested (trimethylalanine, betonicine, ectoine, GBT, L-carnitine, propionobetaine and trigonelline) enhanced cellular ATP (Fig. 3). Unlike HTCC1062, ATP was not elevated by DMSP addition with strain HTCC7211 (Fig. 3). There is only one gene in HTCC7211 genomes that has any similarity to DMSP lyases, *dddP*, and that enzyme, when cloned into *E. coli*, had minimal DMSP lyase activity (Sun *et al*., 2016).

Pyruvate substitutions. We also explored the role of the significant competitor compounds from Fig. 2 in the growth of *Pelagibacter* cells as substitutes for glycine or pyruvate. As mentioned previously, *Pelagibacter* cells are incapable of synthesizing glycine, while pyruvate is required in *Pelagibacter* growth partially for its use as an alanine source, as they are incapable of synthesizing alanine (Carini *et al*., 2013). However, alanine alone does not substitute for pyruvate, indicating that SAR11 cells require pyruvate also for its use in central carbon metabolism (Carini *et al*., 2013).

In HTCC1062, five compounds (trimethylalanine, betonicine, L-carnitine, trigonelline and ectoine) were strong pyruvate substitutes, yielding both growth rate and maximum cell densities significantly higher than in the negative control (Fig. 4). The canonical metabolic pathways for four of these five compounds, excluding trimethylalanine, produce pyruvate precursors or pyruvate itself. L-carnitine is known to be metabolized into malate, a pyruvate precursor and trimethylamine (TMA) in *Acinetobacter baumannii* (Wargo and Meadows, 2015). Malate alone is not able to substitute for pyruvate in HTCC1062 cells (Carini *et al*., 2013), but TMA is known to be used as an ATP source by HTCC1062 via tetrahydrofolate-mediated oxidation (Sun *et al*., 2011), which could explain why L-carnitine is a pyruvate substitute but malate alone is not. Similarly, trigonelline is known to be metabolized to malate by rhizobacteria via nicotinic acid (Joshi and Handler, 1962; Jimenez *et al*., 2008), but none of the genes responsible for this metabolic pathway have homologues in either species of *Pelagibacter.* Ectoine is known to be converted into L-aspartate, an oxaloacetate precursor, in *Halomonas elongate* (Schwibbert *et al*., 2011). Oxaloacetate is able to fully substitute for pyruvate in HTCC1062 (Carini *et al*., 2013). Betonicine is known to be metabolized to glyoxylate and pyruvate in eukaryotes (Watanabe *et al*., 2012). Glyoxylate is predicted to be converted into glycine in HTCC1062 when cellular glycine levels are low (Carini *et al*., 2013), which would explain the weak glycine substitution observed with addition of betonicine (Fig. 4).

For ectoine and L-carnitine, there are homologues in HTCC1062 and HTCC7211 for almost all the necessary enzymes in canonical catabolic pathways, with over 90% cover and above 25% identity. For betonicine and trigonelline, there are few or no homologues, respectively, for the canonical catabolic pathways. To our knowledge, there is no canonical metabolic pathway for trimethylalanine. Since trimethylalanine differs from alanine by only a few methyl groups, we speculate that there may be an enzyme in HTCC1062 capable of demethylating trimethylalanine to alanine, supplying cells with their required alanine source as well as a source of energy from oxidizing the cleaved methyl groups. On the other hand, HTCC1062 cells did not appear

to produce ATP from trimethylalanine (see Fig. 3). It is possible that HTCC1062 cells use the methyl groups from trimethylalanine in methionine regeneration instead, as they do with the first methyl group from GBT (Sun *et al*., 2011).

Unexpectedly, in HTCC7211, none of the compounds tested were able to substitute for pyruvate, with betonicine alone a weak pyruvate substitute (see Fig. 4). There are no genetic differences between the two strains in the pyruvate metabolism pathways that would explain the observed difference.

Glycine substitutions. In both strains of SAR11, GBT was able to substitute for glycine (see Fig. 4); the growth rate of HTCC1062 with GBT as a glycine source that was observed in this paper (0.28 day^{-1}) is somewhat higher than those observed before (0.18 day^{-1}) (Carini *et al*., 2013), but was still lower than the positive control (0.36 day^{-1}) (Fig. 4). The two strains of SAR11 were able to substitute several other compounds for glycine, although most (butyrobetaine and betonicine in HTCC1062; L-carnitine and trimethylalanine in HTCC7211) were weak substitutes (only growth rate significantly higher than negative control, not maximum cell density), with propionobetaine alone being the only other strong glycine substitute, and only in HTCC1062. The metabolic pathway for propionobetaine is a mystery. The predicted metabolic pathway for betonicine as a glycine source in HTCC1062 is discussed above. It is not clear why betonicine is not a glycine substitute in HTCC7211 also, as all the homologous genes in the betonicine metabolic pathway in HTCC1062 are also present in HTCC7211. The other three compounds that were glycine substitutes, butyrobetaine in HTCC1062 and trimethylalanine and L-carnitine in HTCC7211, were all weak glycine substitutes, with no clear genetic differences between the two strains that would explain the differential use of the three compounds. The differences in growth rates and maximum cell densities between these treatments and the negative controls were so slight (although still statistically significant) that it is doubtful whether these compounds are truly substituting for glycine in these two strains (Supporting Information Tables S3 and S4).

Butyrobetaine, proline betaine and L-pipecolate were the three competitor compounds that were not glycine or pyruvate substitutes in either strain (except butyrobetaine as a weak glycine substitute in HTCC1062) and were not used to produce ATP (except, perhaps, proline betaine by HTCC1062). It is possible that these compounds are used in other ways by the cells, maybe as osmolytes, as the native osmolytes used by SAR11 cells for osmoprotection are unknown. All three compounds are known be used as an osmolyte or oxidized by cells (Rajagopal Rao and Rodwell, 1962; Gouesbet *et al*., 1994; Amin *et al*., 1995; Wargo and Meadows, 2015). It is odd that proline betaine, which is structurally similar to betonicine, was not metabolized by SAR11 cells. It is also odd that butyrobetaine was not utilized as an ATP source by both strains, as both strains of *Pelagibacter* have a homologue for the enzyme for converting butyrobetaine into L-carnitine, gamma-butyrobetaine dioxygenase. It is possible that these homologues in these two strains have a different function and are not capable of converting butyrobetaine into L-carnitine.

Overall, out of the 10 competitor compounds, seven are clearly being metabolized by both strains of SAR11: trimethylalanine, betonicine, DMSP (only in HTCC1062), ectoine, L-carnitine, propionobetaine and trigonelline. Trimethylalanine, betonicine, ectoine, L-carnitine and trigonelline are used by HTCC1062 as pyruvate sources, propionobetaine is used by HTCC1062 as a glycine source, and DMSP is used by HTCC1062 as a reduced sulfur source. This metabolic data adds to the picture of SAR11 cells as scavengers, using a range of compounds to fulfil their complex metabolic requirements.

Differential proX specificity between HTCC1062 and HTCC7211. The observed different substrate specificities of the *proXYZ* transporters in HTCC1062 and HTCC7211 may not be significant; three of the four compounds that were competitors in HTCC1062 but not in HTCC7211 were used by HTCC7211 cells, as indicated by the increase in ATP in the trimethylalanine, L-carnitine and betonicine treatments in HTCC7211 ATP assays (Fig. 3). Although there are conserved differences between SAR11 subgroup 1a.1 and 1a.3 *proX* sequences, they do not appear to correlate with residues involved in substrate binding (Supporting Information Fig. S3). However, the SWISS-MODEL alignment of the HTCC1062 *proX* protein with the template had only 18% similarity, so until the actual structures of the *proX* proteins in HTCC1062 and HTCC7211 are determined, it is impossible to be certain. There are no known transporters for trimethylalanine or betonicine, and the only known transporter for L-carnitine, OpuC in *Listeria monocytogenes* (Fraser *et al*., 2000), has no homology to HTCC7211 genes. Thus, it is most likely that these three compounds were transported via the *proXYZ* transporter in HTCC7211, but their competition with GBT was low enough that it was not detected in our competition assay, a problem that could be addressed by increasing the concentration of these three competitor compounds relative to the ^{14}C-GBT in future experiments.

Conclusion. A recent report estimates that SAR11 cells consume up to 37% of Gross Ocean Primary Production (White *et al*., 2019), raising anew the question of how these cells achieve success with minimal genomes. Here, we report that *Pelagibacter* transporter kinetic properties favour competitive success at the low end of substrate

concentrations, a strategy that Tilman (1981) proposed could lead to competitive displacement of organisms with less advantageous transport characteristics. Paradoxically, minimization of cell size contributes to maximization of specific affinity (Flynn *et al*., 2018), while in principle decreasing the range of substrates a cell can use and the rate at which those substrates can be metabolized. Accumulating evidence suggests that *Pelagibacter* cells have evolved to retain a competitive edge at the extremes of oligotrophy while sacrificing a minimum in substrate range.

The experiments presented here were done with two strains of SAR11, using compounds transported by a single transport system, under conditions that are different from what cells may experience in the open ocean. However, the close alignment of the K_s values we measured with those measured by Kiene *et al*. (1998) in seawater with GBT as the substrate suggest that this controlled living system is a good example of the transport systems that dominate DOM transport in the oceans in the range of ambient oligotrophic conditions. These experiments mark several competitor compounds as potentially important forms of labile, DOM. Environmental concentrations for most of these compounds, including GBT, have not been measured in the ocean, with the exception of DMSP, which is found in low nanomolar concentrations (Turner *et al*., 1995; Kiene and Linn, 2000). These compounds may constitute an important part of the labile DOC pool, but that remains unknown since sources, sinks and rates of utilization for many of these compounds are unmeasured.

It seems likely that the kinetic parameters we measured in *Pelagibacter* cells will be assimilated into ecological models (Vallino *et al*., 1996; Vallino, 2000; Payn *et al*., 2014; Reinhold *et al*., 2019) and theoretical models (Hellweger, 2018). Kinetic parameters such as K_s and a^o_s determine rates of DOM utilization by bacteria, which in turn constrain the growth rates of cells in models. Such models, when populated with realistic numbers determined experimentally, have promise for advancing our understanding of how cells evolve to compete at extremely low nutrient environments. Such oligotrophic environments are becoming more common in the oceans as they warm.

Experimental procedures

Growth and washing of cultures. Candidatus Pelagibacter sp. HTCC7211 and *C.* P. ubique HTCC1062 cultures were started from frozen 10% glycerol stocks and grown to mid-exponential phase at 20°C or 16°C, respectively, in 12 h light/dark cycles on sterile artificial seawater (ASW) amended with 100 μM pyruvate, 50 μM glycine, 10 μM methionine and 1× vitamin mix (Carini *et al*., 2013). Cells were then pelleted via centrifugation on a Beckman J2-21 Centrifuge at 10°C at 30 000*g* for 90 min, followed by washing in ASW with no added organics in a Beckman-Coulter Ultracentrifuge at 12°C at 48 000 g for 60 min (Sun *et al*., 2016). The cell pellets were re-suspended in un-amended ASW to the final volume and cell density needed for the experiment.

Kinetic experiments. Washed cells were re-suspended in un-amended ASW to a final concentration between 4 and 7E6 cells mL^{-1}. Cells were incubated for 2 h in the original incubation conditions to allow cells to remove any intracellular stores of nutrients or extracellular traces of organics. Then, the culture was subdivided into the volume needed for detection of uptake at the concentration being used in those cultures. Aliquoted cells were placed either on ice or at 4°C (HTCC1062 and HTCC7211 respectively) to slow metabolic activity. ^{14}C-GBT (obtained from American Radiolabeled Chemicals, ARC 0748–50 μCi) was added to the cultures at the desired final concentration. Cultures were then incubated for 0, 5 or 10 min at either 16°C or 20°C (HTCC1062 or HTCC7211) in a water bath in the dark. Incubation times were kept short to minimize the effects of intracellular feedback mechanisms (Flynn *et al*., 2018). HTCC7211 cells were warmed at 20°C for 10 min prior to addition of ^{14}C-GBT, as this was found to maximize uptake (data not shown). Killed-cell controls for each concentration of ^{14}C-GBT had 0.1% (v/v) final concentration formaldehyde added, followed by 1-h incubation to ensure all cells were killed before addition of ^{14}C-GBT. Killed-cell controls showed no uptake. A portion of the killed-cell controls was removed to count the total ^{14}C activity added.

Once the incubations were complete, uptake was stopped via addition of 10 mM sodium azide and placement on ice (Sun *et al*., 2016). Cultures were then filtered on 0.1 μm PTFE Omnipore Membrane filters; vacuum was kept < 10 in Hg to minimize cell lysis (Kiene *et al*., 1998). Filters were washed three times with 3 ml of un-amended ASM to remove extracellular ^{14}C-GBT. Filters were then placed in scintillation vials with 5 ml of scintillation fluid (Ultima Gold XR, Perkin Elmer) and stored in the dark for at least 18 h prior to counting on a Beckman Coulter LS 6500 Scintillation Counter (Halsey *et al*., 2012). Raw data from a blank filter was subtracted from each sample, and then the measured counts were converted into units of μg mg $cell^{-1}$ using a cell biomass (dry weight) of 11.9 fg per cell, converted into 35.7 fg wet weight per cell using a conversion factor of 3 g wet weight g dry $weight^{-1}$ (Button, 1998; Cermak *et al*., 2017). Uptake rates (V) were calculated using the R software environment (R Core Team) by fitting a linear regression line to the averages of time points; if the regression line had an R^2 value less than 0.95, data from that concentration was discarded. Non-linear regression

was used to fit the Michaelis–Menten equation to a plot of V versus S (Greco and Hakala, 1979).

Kinetic data from the literature were converted into mg wet weight for cell biomass using the following conversion factors: 5.7 g wet weight g protein^{-1}, and 0.55 g carbon g dry weight^{-1} (Martens-Habbena *et al*., 2009). Specific affinities were calculated from the formula V_{max}/K_s, where V_{max} is the maximal uptake rate (nmol S mg cells^{-1} h^{-1}) and K_s is the half-saturation constant (nM) (Button *et al*., 2004).

Competition assay. Following washing as described above, cells were re-suspended in un-amended ASM and incubated for 1 h in the original incubation conditions. Cells were then divided into 5 ml aliquots and metabolic activity slowed as described above. Cultures were removed from ice or 4°C in triplicate and 100 nM final concentration of an unlabeled competitor compound was added (see Table 1 for a list of competitors used), followed by 25 nM final concentration ^{14}C-GBT. A 'None' control treatment had no competitor compound added. Unlabeled GBT was used as a positive control competitor and glucose as a negative control competitor, as glucose does not use the same transporter as GBT (Azam and Hodson, 1981). Following addition of ^{14}C-GBT and competitor, cultures were incubated for 10 min at either 16°C or 20°C (HTCC1062 or HTCC7211 respectively) in a water bath in the dark. Two separate triplicate sets of 'None' controls were run, one at the beginning and one at the end of the experiment, to identify drift (decreases in uptake of ^{14}C-GBT) caused by time on ice or at 4°C, presumably due to decreasing activity of cells. In cases where uptake in the second set differed more than 30% from the first set, all samples, except those run simultaneously with the control cultures, were discarded. Killed-cell controls were used as described above, and uptake of ^{14}C-GBT was detected as detailed above using liquid scintillation.

Uptake in the competitor treatments was calculated as a percentage of the uptake in the 'None' control. A one-sided Dunnett's Test for comparing multiple treatments against a single control was used ($P < 0.05$) as a more powerful method for detecting differences between the treatment groups and the control than other multiple-comparison procedures (Dunnett, 1955; Lee and Lee, 2018). A one-sided test was used instead of two-sided, because we were testing for reduction of uptake by the competitor compounds. The glucose negative control was used as the negative control to account for lowering of ^{14}C-GBT uptake due to non-competitive reasons.

Competitor compounds were picked based off their structural similarity to GBT, their use in similar competition experiments in other similar experiments (Jebbar *et al*., 1992; Gouesbet *et al*., 1996; Kiene *et al*., 1998) and their general properties as osmolytes (Burg and Ferraris, 2008; Vit *et al*., 2015) and represent a subsample of all possible competitor compounds.

ATP assay. The procedure used for the ATP assays was adapted from Sun *et al*., 2011. Briefly, HTCC1062 and HTCC7211 cultures were grown as described above. The 11 competitor compounds found to be significant from the competition assay (including GBT) were added at a final concentration of 100 nM in early log phase to batch cultures to acclimate cells to the compounds, similar to Sun *et al*. (2011). When the test compounds were added at the beginning of growth, cultures did not grow up to the requisite cell densities. At early stationary phase, cultures were washed as described above and re-suspended in ASM with 1× vitamin mix added and then split into 300 μl portions. Cultures were starved for 20 h in the dark at the original incubation temperature prior to addition of the treatment compound in triplicate cultures. For the negative control treatment, nothing was added; for positive control, 100 μM pyruvate (the concentration added to cultures during normal growth) was added to check for metabolic activity of cells.

All competitors were added at 1 μM final concentration, as used in similar ATP experiments (Sun *et al*., 2011; Halsey *et al*., 2012). For propionobetaine, proline betaine, L-pipecolate and butyrobetaine, addition of 1 μM of those compounds resulted in decreases in ATP contents in cells, implying they are inhibitory to SAR11 growth at high concentrations. The concentrations of these four compounds were lowered until no inhibition of ATP production was observed (100 nM final concentration). Cells were incubated for 5 h in the dark at original incubation temperatures following additions of compounds. ATP contents were measured using a luciferase-based assay (BactTiter Glo, Promega, Madison, WI) by adding 20 μl of culture to 90 μl of BactTiterGlo reagent in a white 96-well plate (Tissue culture-treated, Falcon, Corning, NY) and running on a multi-functional plate reader (TECAN, Infinite M200) after 3 s shaking and 4 min waiting time, using 1 s integration and 10 ms settle time. An ATP standard curve using standards in ASW was used to calculate the concentration of ATP in the samples. As in the competition assay, a one-sided Dunnett's test ($P < 0.05$) was used to detect significant increases in ATP content in the experimental treatments compared to the negative control.

Growth experiments. Growth experiments were conducted to determine if the competitor compounds found to be significant from the competition assay were used by HTCC1062 and HTCC7211 as either a pyruvate or glycine source. Washed cells were grown with the same media as described above, except without pyruvate or

glycine. Test compounds were initially added at 50 μM final concentration, which is roughly the concentrations of pyruvate or glycine usually used for growing these cells. For many of the compounds (proline betaine, ectoine, trigonelline, L-pipecolate, butyrobetaine and propionobetaine), 50 μM final concentration caused inhibition of growth (lower growth than the negative control) in both strains. Thus, the concentrations for those compounds were lowered until no inhibition of growth was observed (100 nM final concentration). 1 μM GBT was used as in previous experiments (Sun *et al*., 2011; Carini *et al*., 2013). Negative controls were included lacking either pyruvate or glycine, and a positive control with both pyruvate and glycine.

Triplicates of each treatment were grown at 16°C or 20°C (HTCC1062 or HTCC7211 respectively) in 12 h light/12 h dark. Cell counts were measured twice a week and growth rates were calculated as described elsewhere (Carini *et al*., 2013). The maximum cell densities and growth rates of the triplicate experimental treatments were averaged and compared with the negative controls using a one-sided Dunnett's test (as explained previously) to detect significant increases in maximum cell density or growth rate compared to the negative control ($P < 0.05$).

Bioinformatics. Amino acid sequences for *proX* genes from SAR11 genomes were downloaded using Geneious and an MSA generated using the Clustal Omega webserver, with the results visualized using the MView webserver (Brown *et al*., 1998; McWilliam *et al*., 2013; Sievers *et al*., 2014; Li *et al*., 2015). An RaxML tree was constructed using an MAFT alignment of the sequences. To visualize the conserved amino acid differences between the two subgroups of SAR11, the *proX* amino acid sequence for HTCC1062 and HTCC7211 were searched against the SWISS-MODEL database (Guex *et al*., 2009; Benkert *et al*., 2011; Bertoni *et al*., 2017; Bienert *et al*., 2017; Waterhouse *et al*., 2018). The top model for both sequences, the GBT-substrate binding protein from *E. coli*, was used to visualize the differential amino acid sites.

Acknowledgements

The authors would like to thank Dr. Jing Sun for her assistance with experimental methods and advice about the uptake experiments, and the Schuster lab for allowing use of their luminometer equipment. The authors would also like to thank Dr. Jonathan D. Todd for kindly providing the DMSP and O. Muslin for providing the propionobetaine used in these experiments. The authors are grateful to Dr. Chris Suffridge for comments and feedback on the paper. The authors declare no competing financial interests. This work was funded by the National Science Foundation grants OCE-1436865 and IOS- 1838445.

References

Amin, U.S., Lash, T.D., and Wilkinson, B.J. (1995) Proline betaine is a highly effective osmoprotectant for *Staphylococcus aureus*. *Arch Microbiol* **163**: 138–142.

Azam, F., and Hodson, R.E. (1981) Multiphasic kinetics for D-glucose uptake by assemblages of natural marine bacteria. *Mar. Ecol.* **6**: 213–222.

Benkert, P., Biasini, M., and Schwede, T. (2011) Toward the estimation of the absolute quality of individual protein structure models. *Bioinformatics* **27**: 343–350.

Bertoni, M., Kiefer, F., Biasini, M., Bordoli, L., and Schwede, T. (2017) Modeling protein quaternary structure of homo- and hetero-oligomers beyond binary interactions by homology. *Sci Rep* **7**: 10480.

Bienert, S., Waterhouse, A., de Beer, T.A.P., Tauriello, G., Studer, G., Bordoli, L., and Schwede, T. (2017) The SWISS-MODEL repository—new features and functionality. *Nucleic Acids Res* **45**: D313–D319.

Bosdriesz, E., Magnúsdóttir, S., Bruggeman, F.J., Teusink, B., and Molenaar, D. (2015) Binding proteins enhance specific uptake rate by increasing the substrate-transporter encounter rate. *FEBS J* **282**: 2394–2407.

Brown, N.P., Leroy, C., and Sander, C. (1998) MView: a web-compatible database search or multiple alignment viewer. *Bioinformatics* **14**: 380–381.

Brown, M.V., Lauro, F.M., DeMaere, M.Z., Muir, L., Wilkins, D., Thomas, T., *et al*. (2012) Global biogeography of SAR11 marine bacteria. *Mol Syst Biol* **8**: 595.

Burg, M.B., and Ferraris, J.D. (2008) Intracellular organic Osmolytes: function and regulation. *J Biol Chem* **283**: 7309–7313.

Button, D.K. (1998) Nutrient uptake by microorganisms according to kinetic parameters from theory as related to Cytoarchitecture. *Microbiol Mol Biol Rev* **62**: 636–645.

Button, D.K., Robertson, B.R., Lepp, P.W., and Schmidt, T. M. (1998) A small, dilute-cytoplasm, high-affinity, novel bacterium isolated by extinction culture and having kinetic constants compatible with growth at ambient concentrations of dissolved nutrients in seawater. *Appl Environ Microbiol* **64**: 4467–4476.

Button, D.K., Robertson, B., Gustafson, E., and Zhao, X. (2004) Experimental and theoretical bases of specific affinity, a cytoarchitecture-based formulation of nutrient collection proposed to supercede the Michaelis-Menten paradigm of microbial kinetics. *Appl Environ Microbiol* **70**: 5511–5521.

Carini, P., Steindler, L., Beszteri, S., and Giovannoni, S.J. (2013) Nutrient requirements for growth of the extreme oligotroph "*Candidatus* Pelagibacter ubique"HTCC1062 on a defined medium. *ISME J* **7**: 592–602.

Carini, P., Campbell, E.O., Morré, J., Sañudo-Wilhelmy, S.A., Thrash, J.C., Bennett, S.E., *et al*. (2014) Discovery of a SAR11 growth requirement for thiamin's pyrimidine precursor and its distribution in the Sargasso Sea. *ISME J* **8**: 1727–1738.

Cermak, N., Becker, J.W., Knudsen, S.M., Chisholm, S.W., Manalis, S.R., and Polz, M.F. (2017) Direct single-cell biomass estimates for marine bacteria via Archimedes' principle. *ISME J* **11**: 825–828.

Choquet, G., Jehan, N., Pissavin, C., Blanco, C., and Jebbar, M. (2005) OusB, a broad-specificity ABC-type transporter from Erwinia chrysanthemi, mediates uptake of

glycine betaine and choline with a high affinity. *Appl Environ Microbiol* **71**: 3389–3398.

Clifford, E.L., Hansell, D.A., Varela, M.M., Nieto-Cid, M., Herndl, G.J., and Sintes, E. (2017) Crustacean zooplankton release copious amounts of dissolved organic matter as taurine in the ocean: dissolved free taurine in oceanic waters. *Limnol Oceanogr* **62**: 2745–2758.

Curson, A.R.J., Liu, J., Bermejo Martínez, A., Green, R.T., Chan, Y., Carrión, O., *et al*. (2017) Dimethylsulfoniopropionate biosynthesis in marine bacteria and identification of the key gene in this process. *Nat Microbiol* **2**: 17009.

Dadon-Pilosof, A., Conley, K.R., Jacobi, Y., Haber, M., Lombard, F., Sutherland, K.R., *et al*. (2017) Surface properties of SAR11 bacteria facilitate grazing avoidance. *Nat Microbiol* **2**: 1608–1615.

Davidson, A.L., Dassa, E., Orelle, C., and Chen, J. (2008) Structure, function, and evolution of bacterial ATP-binding cassette systems. *Microbiol Mol Biol Rev* **72**: 317–364.

Diaz, M.R., Visscher, P.T., and Taylor, B.F. (1992) Metabolism of dimethylsulfoniopropionate and glycine betaine by a marine bacterium. *FEMS Microbiol Lett* **96**: 61–65.

Dunfield, P.F., Liesack, W., Henckel, T., Knowles, R., and Conrad, R. (1999) High-affinity methane oxidation by a soil enrichment culture containing a type II methanotroph. *Appl Environ Microbiol* **65**: 1009–1014.

Dunnett, C.W. (1955) A multiple comparison procedure for comparing several treatments with a control. *J Am Stat Assoc* **50**: 1096–1121.

Eren, A.M., Maignien, L., Sul, W.J., Murphy, L.G., Grim, S.L., Morrison, H.G., and Sogin, M.L. (2013) Oligotyping: differentiating between closely related microbial taxa using 16S rRNA gene data. *Methods Ecol Evol* **4**: 1111–1119.

Ferla, M.P., Brewster, J.L., Hall, K.R., Evans, G.B., and Patrick, W.M. (2017) Primordial-like enzymes from bacteria with reduced genomes: primordial-like bacterial enzymes. *Mol Microbiol* **105**: 508–524.

Fischer, E. (1894) Einfluss der Configuration auf die Wirkung der Enzyme. *Berichte Dtsch Chem Ges* **27**: 2985–2993.

Flynn, K.J. (1998) Estimation of kinetic parameters for the transport of nitrate and ammonium into marine phytoplankton. *Mar Ecol Prog Ser* **169**: 13–28.

Flynn, K.J., Skibinski, D.O.F., and Lindemann, C. (2018) Effects of growth rate, cell size, motion, and elemental stoichiometry on nutrient transport kinetics. *PLoS Comput Biol* **14**: e1006118.

Fraser, K.R., Harvie, D., Coote, P.J., and O'Byrne, C.P. (2000) Identification and characterization of an ATP binding cassette L-carnitine transporter in *Listeria monocytogenes*. *Appl Environ Microbiol* **66**: 4696–4704.

Giovannoni, S.J. (2005) Genome streamlining in a cosmopolitan oceanic bacterium. *Science* **309**: 1242–1245.

Giovannoni, S.J. (2017) SAR11 bacteria: the Most abundant plankton in the oceans. *Ann Rev Mar Sci* **9**: 231–255.

Giovannoni, S.J., Halsey, K.H., Saw, J., Muslin, O., Suffridge, C.P., Sun, J., *et al*. (2019) A parasitic arsenic cycle that shuttles energy from phytoplankton to heterotrophic bacterioplankton. *mBio* **10**: e00246–19.

Gouesbet, G., Jebbar, M., Talibart, R., Bernard, T., and Blanco, C. (1994) Pipecolic acid is an osmoprotectant for *Escherichia coli* taken up by the general osmoporters ProU and ProP. *Microbiology* **140**: 2415–2422.

Gouesbet, G., Trautwetter, A., Bonnassie, S., Wu, L.F., and Blanco, C. (1996) Characterization of the Erwinia chrysanthemi osmoprotectant transporter gene ousA. *J Bacteriol* **178**: 447–455.

Graham, L.L., Beveridge, T.J., and Nanninga, N. (1991) Periplasmic space and the concept of the periplasm. *Trends Biochem Sci* **16**: 328–329.

Grant, S.C., and Blackband, S.J. (2002) Osmolyte distribution and diffusion in isolated single neurons. *Proc Int Soc Magn Reson Med* **10**.

Greco, W., and Hakala, M. (1979) Evaluation of methods for estimating the dissociation constant of tight binding enzyme inhibitors. *J Biol Chem* **254**: 12104–12109.

Green, R., Hanfrey, C.C., Elliott, K.A., McCloskey, D.E., Wang, X., Kanugula, S., *et al*. (2011) Independent evolutionary origins of functional polyamine biosynthetic enzyme fusions catalysing de novo diamine to triamine formation: polyamine enzyme fusions. *Mol Microbiol* **81**: 1109–1124.

Guex, N., Peitsch, M.C., and Schwede, T. (2009) Automated comparative protein structure modeling with SWISS-MODEL and Swiss-PdbViewer: a historical perspective. *Electrophoresis* **30**: S162–S173.

Halsey, K.H., Carter, A.E., and Giovannoni, S.J. (2012) Synergistic metabolism of a broad range of C1 compounds in the marine methylotrophic bacterium HTCC2181: C1 metabolism in the marine isolate HTCC2181. *Environ Microbiol* **14**: 630–640.

Halsey, K.H., Giovannoni, S.J., Graus, M., Zhao, Y., Landry, Z., Thrash, J.C., *et al*. (2017) Biological cycling of volatile organic carbon by phytoplankton and bacterioplankton: VOC cycling by marine plankton. *Limnol Oceanogr* **62**: 2650–2661.

Hellweger, F.L. (2018) Heterotrophic substrate specificity in the aquatic environment: the role of microscale patchiness investigated using modelling: substrate specificity and microscale patchiness. *Environ Microbiol* **20**: 3825–3835.

Hoffmann, T., and Bremer, E. (2017) Guardians in a stressful world: the Opu family of compatible solute transporters from Bacillus subtilis. *Biol Chem* **398**: 193–214.

Hosie, A.H.F., Allaway, D., Galloway, C.S., Dunsby, H.A., and Poole, P.S. (2002) Rhizobium leguminosarum has a second general amino acid permease with unusually broad substrate specificity and high similarity to branched-chain amino acid transporters (bra/LIV) of the ABC family. *J Bacteriol* **184**: 4071–4080.

Jebbar, M., Talibart, R., Gloux, K., Bernard, T., and Blanco, C. (1992) Osmoprotection of *Escherichia coli* by ectoine: uptake and accumulation characteristics. *J Bacteriol* **174**: 5027–5035.

Jimenez, J.I., Canales, A., Jimenez-Barbero, J., Ginalski, K., Rychlewski, L., Garcia, J.L., and Diaz, E. (2008) Deciphering the genetic determinants for aerobic nicotinic acid degradation: the nic cluster from pseudomonas putida KT2440. *Proc Natl Acad Sci* **105**: 11329–11334.

Joshi, J.G., and Handler, P. (1962) Metabolism of Trigonelline. *J Biol Chem* **237**: 3185–3188.

Kelkar, Y.D., and Ochman, H. (2013) Genome reduction promotes increase in protein functional complexity in bacteria. *Genetics* **193**: 303–307.

Keller, M.D., Kiene, R.P., Matrai, P.A., and Bellows, W.K. (1999) Production of glycine betaine and dimethylsulfoniopropionate in marine phytoplankton. I. Batch cultures. *Mar Biol* **135**: 237–248.

Kiene, R.P., and Linn, L.J. (2000) Distribution and turnover of dissolved DMSP and its relationship with bacterial production and dimethylsulfide in the Gulf of Mexico. *Limnol Oceanogr* **45**: 849–861.

Kiene, R.P., and Williams, L.P.H. (1998) Glycine betaine uptake, retention, and degradation by microorganisms in seawater. *Limnol Oceanogr* **43**: 1592–1603.

Kiene, R.P., Hoffmann Williams, L.P., and Walker, J.E. (1998) Seawater microorganisms have a high affinity glycine betaine uptake system which also recognizes dimethylsulfoniopropionate. *Aquat Microb Ecol* **15**: 39–51.

King, G.M. (1984) Metabolism of trimethylamine, choline, and glycine betaine by sulfate-reducing and methanogenic bacteria in marine sediments. *Appl Environ Microbiol* **48**: 719–725.

Koch, A.L., and Wang, C.H. (1982) How close to the theoretical diffusion limit do bacterial uptake systems function? *Arch Microbiol* **131**: 36–42.

Lee, C., and Bada, J.L. (1977) Dissolved amino acids in the equatorial Pacific, the Sargasso Sea, and Biscayne Bay1: seawater dissolved amino acids. *Limnol Oceanogr* **22**: 502–510.

Lee, S., and Lee, D.K. (2018) What is the proper way to apply the multiple comparison test? *Korean J Anesthesiol* **71**: 353–360.

Lendenmann, U., Snozzi, M., and Egli, T. (1996) Kinetics of the simultaneous utilization of sugar mixtures by *Escherichia coli* in continuous culture. *Appl Environ Microbiol* **62**: 1493–1499.

Li, W., Cowley, A., Uludag, M., Gur, T., McWilliam, H., Squizzato, S., *et al*. (2015) The EMBL-EBI bioinformatics web and programmatic tools framework. *Nucleic Acids Res* **43**: W580–W584.

Lidbury, I., Murrell, J.C., and Chen, Y. (2014) Trimethylamine N-oxide metabolism by abundant marine heterotrophic bacteria. *Proc Natl Acad Sci* **111**: 2710–2715.

Lu, X., Zou, L., Clevinger, C., Liu, Q., Hollibaugh, J.T., and Mou, X. (2014) Temporal dynamics and depth variations of dissolved free amino acids and polyamines in coastal seawater determined by high-performance liquid chromatography. *Mar Chem* **163**: 36–44.

Lucht, J.M., and Bremer, E. (1994) Adaptation of *Escherichia coli* to high osmolarity environments: osmoregulation of the high-affinity glycine betaine transport system ProU. *FEMS Microbiol Rev* **14**: 3–20.

Martens-Habbena, W., Berube, P.M., Urakawa, H., de la Torre, J.R., and Stahl, D.A. (2009) Ammonia oxidation kinetics determine niche separation of nitrifying archaea and bacteria. *Nature* **461**: 976–979.

McWilliam, H., Li, W., Uludag, M., Squizzato, S., Park, Y.M., Buso, N., *et al*. (2013) Analysis tool web services from the EMBL-EBI. *Nucleic Acids Res* **41**: W597–W600.

Morris, R.M., Rappé, M.S., Connon, S.A., Vergin, K.L., Siebold, W.A., Carlson, C.A., and Giovannoni, S.J. (2002) SAR11 clade dominates ocean surface bacterioplankton communities. *Nature* **420**: 806–810.

Nicastro, D., Schwartz, C., Pierson, J., Cho, J.-C., Giovannoni, S., and McIntosh, J. (2006) Three-dimensional structure of the tiny bacterium *Pelagibacter ubique* studied by cryo-electron tomography. *Microsc Microanal* **12**: 180–181.

Nissen, H., Nissen, P., and Azam, F. (1984) Multiphasic uptake of D-glucose by an oligotrophic marine bacterium. *Mar Ecol* **16**: 155–160.

Obernosterer, I., Kraay, G., de Ranitz, E., and Herndl, G. (1999) Concentrations of low molecular weight carboxylic acids and carbonyl compounds in the Aegean Sea (Eastern Mediterranean) and the turnover of pyruvate. *Aquat Microb Ecol* **20**: 147–156.

Payn, R.A., Helton, A.M., Poole, G.C., Izurieta, C., Burgin, A. J., and Bernhardt, E.S. (2014) A generalized optimization model of microbially driven aquatic biogeochemistry based on thermodynamic, kinetic, and stoichiometric ecological theory. *Ecol Model* **294**: 1–18.

R Core Team. (2018) R: A language and environment for statistical computing R Foundation for Statistical Computing, Vienna, Austria. https://www.R-project.org/.

Rajagopal Rao, D., and Rodwell, V.W. (1962) Metabolism of pipecolic acid in a pseudomonas species. *J Biol Chem* **237**: 2232–2238.

Reinhold, A.M., Poole, G.C., Izurieta, C., Helton, A.M., and Bernhardt, E.S. (2019) Constraint-based simulation of multiple interactive elemental cycles in biogeochemical systems. *Ecol Inform* **50**: 102–121.

Robertson, B.R., and Button, D.K. (1979) Phosphate-limited continuous culture of *Rhodotorula rubra*: kinetics of transport, leakage, and growth. *J Bacteriol* **138**: 884–895.

Rudulier, D.L., and Bouillard, L. (1983) Glycine betaine, an osmotic effector in Klebsiella pneumoniae and other members of the Enterobacteriaceae. *Appl Environ Microbiol* **46**: 152–159.

Schiefner, A., Breed, J., Bösser, L., Kneip, S., Gade, J., Holtmann, G., *et al*. (2004) Cation-π interactions as determinants for binding of the compatible solutes glycine betaine and proline betaine by the periplasmic ligand-binding protein ProX from *Escherichia coli*. *J Biol Chem* **279**: 5588–5596.

Schut, F., Jansen, M., Pedro Gomes, T.M., Gottschal, J.C., Harder, W., and Prins, R.A. (1995) Substrate uptake and utilization by a marine ultramicrobacterium. *Microbiology* **141**: 351–361.

Schwibbert, K., Marin-Sanguino, A., Bagyan, I., Heidrich, G., Lentzen, G., Seitz, H., *et al*. (2011) A blueprint of ectoine metabolism from the genome of the industrial producer *Halomonas elongata* DSM 2581^T. *Environ Microbiol* **13**: 1973–1994.

Sievers, F., Wilm, A., Dineen, D., Gibson, T.J., Karplus, K., Li, W., *et al*. (2014) Fast, scalable generation of high-quality protein multiple sequence alignments using Clustal Omega. *Mol Syst Biol* **7**: 539–539.

Sowell, S.M., Norbeck, A.D., Lipton, M.S., Nicora, C.D., Callister, S.J., Smith, R.D., *et al*. (2008) Proteomic analysis of stationary phase in the marine bacterium "*Candidatus* Pelagibacter ubique.". *Appl Environ Microbiol* **74**: 4091–4100.

Sowell, S.M., Wilhelm, L.J., Norbeck, A.D., Lipton, M.S., Nicora, C.D., Barofsky, D.F., *et al*. (2009) Transport

functions dominate the SAR11 metaproteome at low-nutrient extremes in the Sargasso Sea. *ISME J* **3**: 93–105.
Steindler, L., Schwalbach, M.S., Smith, D.P., Chan, F., and Giovannoni, S.J. (2011) Energy starved Candidatus Pelagibacter Ubique substitutes light-mediated ATP production for endogenous carbon respiration. *PLoS One* **6**: e19725.
Sun, J., Steindler, L., Thrash, J.C., Halsey, K.H., Smith, D. P., Carter, A.E., *et al*. (2011) One carbon metabolism in SAR11 pelagic marine bacteria. *PLoS One* **6**: e23973.
Sun, J., Todd, J.D., Thrash, J.C., Qian, Y., Qian, M.C., Temperton, B., *et al*. (2016) The abundant marine bacterium *Pelagibacter* simultaneously catabolizes dimethylsulfoniopropionate to the gases dimethyl sulfide and methanethiol. *Nat Microbiol* **1**: 16065.
Tang, K., Jiao, N., Liu, K., Zhang, Y., and Li, S. (2012) Distribution and functions of TonB-dependent transporters in marine bacteria and environments: implications for dissolved organic matter utilization. *PLoS One* **7**: e41204.
Thurman, E.M. (1985) Amino acids. In *Organic Geochemistry of Natural Waters*. Dordrecht: Springer Netherlands, pp. 151–180.
Tilman, D. (1981) Tests of resource competition theory using four species of Lake Michigan algae. *Ecology* **62**: 802–815.
Turner, S.M., Nightingale, P.D., Broadgate, W., and Liss, P. S. (1995) The distribution of dimethyl sulphide and dimethylsulphoniopropionate in Antarctic waters and sea ice. *Deep Sea Res Part II Top Stud Oceanogr* **42**: 1059–1080.
Vallino, J.J. (2000) Improving marine ecosystem models: use of data assimilation and mesocosm experiments. *J Mar Res* **58**: 117–164.
Vallino, J.J., Hopkinson, C.S., and Hobbie, J.E. (1996) Modeling bacterial utilization of dissolved organic matter: optimization replaces Monod growth kinetics. *Limnol Oceanogr* **41**: 1591–1609.
Verheul, A., Rombouts, F.M., Beumer, R.R., and Abee, T. (1995) An ATP-dependent L-carnitine transporter in *Listeria monocytogenes* Scott A is involved in osmoprotection. *J Bacteriol* **177**: 3205–3212.
Vit, A., Misson, L., Blankenfeldt, W., and Seebeck, F.P. (2015) Ergothioneine biosynthetic methyltransferase EgtD reveals the structural basis of aromatic amino acid betaine biosynthesis. *Chembiochem* **16**: 119–125.
Wargo, M.J., and Meadows, J.A. (2015) Carnitine in bacterial physiology and metabolism. *Microbiology* **161**: 1161–1174.
Watanabe, S., Morimoto, D., Fukumori, F., Shinomiya, H., Nishiwaki, H., Kawano-Kawada, M., *et al*. (2012) Identification and characterization of d-Hydroxyproline dehydrogenase and Δ^{1}-Pyrroline-4-hydroxy-2-carboxylate deaminase involved in novel l-hydroxyproline metabolism of bacteria: METABOLIC CONVERGENT EVOLUTION. *J Biol Chem* **287**: 32674–32688.
Waterhouse, A., Bertoni, M., Bienert, S., Studer, G., Tauriello, G., Gumienny, R., *et al*. (2018) SWISS-MODEL: homology modelling of protein structures and complexes. *Nucleic Acids Res* **46**: W296–W303.
White, A.E., Giovannoni, S.J., Zhao, Y., Vergin, K., and Carlson, C.A. (2019) Elemental content and stoichiometry of SAR11 chemoheterotrophic marine bacteria: SAR11 composition. *Limnol Oceanogr Lett* **4**: 44–51.
Zhao, X., Schwartz, C.L., Pierson, J., Giovannoni, S.J., McIntosh, J.R., and Nicastro, D. (2017) Three-dimensional structure of the ultraoligotrophic marine bacterium "Candidatus Pelagibacter ubique.". *Appl Environ Microbiol* **83**: e02807–16.

Supporting Information

Additional Supporting Information may be found in the online version of this article at the publisher's web-site:

Table S1 Growth data from an experiment to determine if the competitor compounds from the competition assay could substitute for glycine or pyruvate in HTCC1062 growth. Either 100 μM pyruvate or 50 μM glycine, 25 μM methionine, and 1× vitamin mix were added to all cultures, in addition to either 50 μM glycine or 100 μM pyruvate (positive control); or 50 μM trimethylalanine, L-carnitine, or betonicine; or no addition (negative control). Cultures were grown at 16°C in 12 h light/12 h dark. Reported growth rates and maximum cell densities are the average of triplicate cultures ± standard deviation.

Table S2 Growth data from an experiment to determine if the competitor compounds from the competition assay could substitute for glycine or pyruvate in HTCC1062 growth. Either 100 μM pyruvate or 50 μM glycine, 25 μM methionine, and 1× vitamin mix were added to all cultures, in addition to either 50 μM glycine or 100 μM pyruvate (positive control); or 100 nM proline betaine, trigonelline, ectoine, propionobetaine, or L-pipecolate; or 1 μM glycine betaine; or no addition (negative control). Cultures were grown at 16°C in 12 h light/12 h dark. Reported growth rates and maximum cell densities are the average of triplicate cultures ± standard deviation.

Table S3 Growth data from an experiment to determine if the competitor compounds from the competition assay could substitute for glycine or pyruvate in HTCC1062 growth. Either 100 μM pyruvate or 50 μM glycine, 25 μM methionine, and 1× vitamin mix were added to all cultures, in addition to either 50 μM glycine or 100 μM pyruvate (positive control); or 100 nM butyrobetaine; or 1 μM glycine betaine; or no addition (negative control). Cultures were grown at 16°C in 12 h light/12 h dark. Reported growth rates and maximum cell densities are the average of triplicate cultures ± standard deviation. The growth rates of the experimental treatments were compared against the growth rates of the negative control cultures to determine if their growth rate was significantly greater (one-sided Dunnett's test).

Table S4 Growth data from an experiment to determine if the competitor compounds from the competition assay could substitute for glycine or pyruvate in HTCC7211 growth. Either 100 μM pyruvate or 50 μM glycine, 25 μM methionine, and 1× vitamin mix were added to all cultures, in addition to either 50 μM (trimethylalanine, L-carnitine, and betonicine), 1 μM (glycine betaine), or 100 nM (proline betaine, trigonelline, ectoine, propionobetaine, L-pipecolate, and butyrobetaine) of the test compound; or no addition (negative control). Positive control had 100 μM pyruvate and 50 μM glycine added. Cultures were grown at 20°C in 12 h light/12 h dark. Reported growth rates and maximum cell densities are the average of triplicate cultures ± standard deviation. The growth rates of the experimental treatments

were compared against the growth rates of the negative control cultures to determine if their growth rate was significantly greater (one-sided Dunnett's test).

Fig. S1. RaxML tree of *proX* genes from selected SAR11 genomes. Green, SAR11 subgroup 1A.1; Orange, subgroup 1A.3. The *proX* sequence from *Dinoroseobacter shibae* was used as the outgroup. The sequences were aligned with MAFT. The pattern in the tree suggests vertical inheritance of *proX* within the SAR11 clade. AAI between the HTCC7211 and HTCC1062 *proX* genes is 93.4%.

Fig. S2 A multiple-sequence alignment of *proX* genes from SAR11 genomes, aligned using Clustal Omega and visualized using MView. Amino acid residues are coloured by identity.

Fig. S3 Locations of the amino acid residues that differ between the SAR11 subgroups 1a.1 and 1a.3 based on the protein sequence that most closely matches the HTCC1062 *proX* sequence from SWISS-MODEL, 1r9l.1.A (Glycine betaine-binding periplasmic protein from *E. coli*). Red arrows point to the variable residues, which are concentrated in an alpha helix directly below the binding pocket. The red circle is around the position of GBT when bound. The template had 18.6% identity with the HTCC1062 *proX* sequence. A similar alignment with the HTCC7211 *proX* sequence returned similar results. According to the SWISS-MODEL Template Library, there are nine residues that are within 4 Â of the ligand, between 17 and 188. None of these correspond to any of the variable amino acid residues identified above; the variations are concentrated in residues 266–313.

Appendix S1: Supplement Figures